'94 KACC (1994. 10. 17 ~ 20)

# A Method of Compliance Control of Redundant Manipulators

H. R. Choi*, W. K. Chung and Y. Youm
Department of Mechanical Engineering
Pohang University of Science and Technology(POSTECH)
San-31 Hyojadong, Pohang, 790-784, Korea

T. Yoshikawa
Department of Mechanical Engineering
Kyoto University
Kyoto 606, Japan

**Abstract**

A compliance control method of redundant manipulators is presented. This method is based on the new stiffness model, which allows us to modulate accurate joint stiffness of realizing the end effector stiffness to be varied with task requirements. Control model is developed and by implementing the proposed method in a three-dof(degree of freedom) planar redundant manipulator, its effectiveness is validated.

## 1 Introduction

In robot manipulators interacting with environment, the capability of compliance control is prerequisite. Up to now, though a lot of approaches have been proposed, the compliance control is classified into two main categories after all, i.e. hybrid position/force control[1] and impedance control[2]. In this paper, we address the stiffness control issue as one of the impedance control schemes, especially that of redundant manipulators.

The stiffness control was originated from Salisbury[3]. In the case of redundant manipulators, this controller has limitation that the null space is left uncontrolled but the end effector can be stationary in unconstrained situation if joint friction is adequate to keep the null space motion from drifting and dynamic disturbances are assumed to be negligible. On the contrary, if the stiffness controlled manipulator contacts with the environment, that is, static forces are exerted at the end effector, the manipulator can not preserve its configuration any more and collapse. The static force generates some disturbance torque and it makes the joint configuration unstable.

In fact, there have been a lot investigations concerning the stiffness control of redundant manipulators[4-6], and they provide their own method of specifying the joint stiffness corresponding to the given taskspace stiffness. However, they are basically derived from the stiffness model of Salisbury[3], that is, the congruence mapping of stiffnesses[11], and in this model, there is no consideration on the effect of the static force. According to Yi et. al[8] the stiffness characteristics at the joint depends on the direction of end effector force and manipulator configuration, and Mussa-Ivaldi and Hogan[7] derived a stiffness model considering the effect of static force although they didn't touch the stiffness specification at the taskspace. That is, the previous model may not be enough to describe the stiffness relation and the effect of static force is required to be included in the model.

In this paper, we present a new stiffness model derived from static force equilibrium. In this model, the effect of static force is introduced in terms of equivalent stiffness, called *induced stiffness obtained from configuration change and force*(ISOC), and the accurate relation between force and deflection is represented. It lets us know which torque should be imposed to realize the desired stiffness and restoring force at the end effector. Conversely, it makes it possible to evaluate the resultant joint stiffness. Based on the developed stiffness model, we propose a stiffness control scheme, called *orthogonal stiffness decomposition control*(OSDC). OSDC is implemented in a three-dof planar redundant manipulator adopting tendon driven method and its effectiveness is confirmed by conducting several experiments.

*Post doctorate researcher in Yoshikawa laboratory, Kyoto University

## 2 Stiffness Modeling

In this section, we establish the stiffness model describing the relations among taskspace stiffness, joint stiffness and static force. *Kinematic redundancy* is usually used to indicate the excess of actively controlled dof at the joint space with respect to that of the taskspace. Here, the taskspace kinematics is described by $N$-dimensional position vector $\boldsymbol{x} = [\, x_1 \cdots x_N \,]^T$ that specifies the location of the end effector with respect to an absolute coordinate frame. The manipulator configuration is fully described by an $n$-dimensional vector of generalized coordinates $\boldsymbol{q} = [\, q_1 \cdots q_n \,]^T$, and redundancy is expressed by the inequality $N \leq n$. The forward kinematics is a vector map

$$\boldsymbol{x} = \boldsymbol{F}(\boldsymbol{q}), \tag{1}$$

from configuration to end effector position, where $\boldsymbol{F} \in \Re^N$ is a vector function assumed to be twice differentiable in the entire workspace. The differential transformation from joint displacement to end effector displacement is

$$d\boldsymbol{x} = \boldsymbol{J}_{\boldsymbol{q}}(\boldsymbol{q})\, d\boldsymbol{q}, \tag{2}$$

where $\boldsymbol{J}_{\boldsymbol{q}}(\boldsymbol{q}) = \partial \boldsymbol{F}(\boldsymbol{q})/\partial \boldsymbol{q} \in \Re^{N \times n}$ is known as the Jacobian of the manipulator. Assuming the frictional and dynamic forces are compensated for or small enough to be neglected, we can compute joint torque $\boldsymbol{\tau} = [\, \tau_1 \cdots \tau_n \,]^T$ necessary to apply an end effector force $\boldsymbol{f} = [\, f_1 \cdots f_N \,]^T$ according to the static relation

$$\boldsymbol{\tau} = \boldsymbol{J}_{\boldsymbol{q}}^T(\boldsymbol{q})\boldsymbol{f}. \tag{3}$$

Also, it has been found useful to be able to superimpose bias force on the stiffness behavior[3] and thus, we suppose that the manipulator be at static equilibrium with its bias force $\boldsymbol{f}_o$, where we have $\boldsymbol{x}_o = \boldsymbol{F}(\boldsymbol{q}_o)$ and $\boldsymbol{\tau}_o = \boldsymbol{J}_{\boldsymbol{q}}^T(\boldsymbol{q}_o)\boldsymbol{f}_o$. Now, if the manipulator is deflected by $d\boldsymbol{x}$ and going to increase the exerting force by $d\boldsymbol{f}$ as illustrated in Fig. 1, the manipulator should move to another static equilibrium

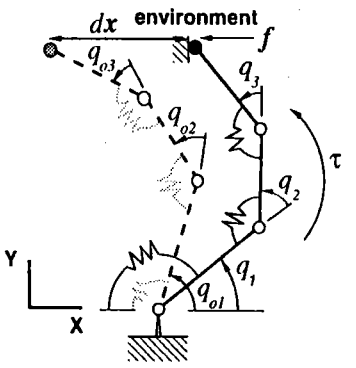


Figure 1: Model of redundant manipulator

at the changed configuration $q_o + dq$ with the changed force $f$ and torque $\tau$ such as

$$\tau = J_q^T(q_o + dq)f \,. \tag{4}$$

Also, the definition of stiffness provides us the following auxiliary stiffness relations.

$$\tau = \tau_o + K_q(q_o - q) \,, \tag{5}$$
$$f = f_o + K_x(x_o - x) \,, \tag{6}$$

where $K_q \in \Re^{n\times n}$ and $K_x \in \Re^{N\times N}$ are the stiffnesses at joint and taskspace, respectively. Differentiating Eqs. (5) and (6), we get

$$d\tau = -K_q dq \,, \tag{7}$$
$$df = -K_x dx \,. \tag{8}$$

The Jacobian matrix at the righthand side of Eq. (4) can be expanded using Taylor series such as

$$J_q^T(q_o + dq) \approx J_q^T(q_o) + \frac{\partial J_q^T(q_o)}{\partial q} dq \,. \tag{9}$$

Substituting Eq. (9) into the right hand side of Eq. (4) yields the result

$$J_q^T(q_o + dq)f = J_q^T(q_o)f + \frac{\partial J_q^T(q_o)}{\partial q} dq f \,. \tag{10}$$

In addition, the last term in the righthand side of Eq. (10) is rearranged as

$$\frac{\partial J_q^T(q_o)}{\partial q} dq f = \Delta(q_o, f) dq \,, \tag{11}$$

where the $i$th row and the $j$th column of $\Delta(q, f)$ is obtained as follows:

$$\Delta(q, f)_{(i,j)} \triangleq \sum_{k=1}^{N} \frac{\partial^2 F_k}{\partial q_i \partial q_j} f_k \,. \tag{12}$$

Using Eqs. (7), (8) and (11), Eq. (4) will be

$$-K_q dq = J_q^T(q_o) df + \Delta(q_o, f) dq \,, \tag{13}$$

and the chain rule gives us

$$df = -K_x J_q(q_o) dq \,. \tag{14}$$

Substituting Eq. (14) into Eq. (13), we get the result

$$K_q = J_q^T(q_o) K_x J_q(q_o) - \Delta(q_o, f) \,. \tag{15}$$

The above Eq. (15) describes how to specify the joint stiffness of realizing the desired taskspace stiffness $K_x$. According to the conventional approaches[3] there is no consideration of $\Delta(q_o, f)$ and the joint stiffness is just determined by the congruence transformation of $K_x$. $\Delta(q_o, f)$ is termed as the *induced stiffness obtained from configuration change and force*(ISOC) in this paper, which is the function of the exerting force and the configuration of the manipulator. Here, note that the exerting force $f$ is the summation of bias force $f_o$ and incremental force $df$ caused by the taskspace stiffness. If $f_o = O$ and $df$ is negligible, Eq. (15) comes to the conventional stiffness model[3]. However, as long as the manipulator is desired to exert controlled force in the reasonable range of motion, ISOC should be taken into account.

Conversely, let us derive the resultant taskspace stiffness for the given joint stiffness $K_q$ and end effector force $f$. Eq. (13) can be reformulated as follows:

$$-[\, K_q + \Delta(q_o, f)\,] dq = J_q^T(q_o) df \,. \tag{16}$$

Assuming that Det $[\, K_q + \Delta(q_o, f)\,] \neq 0$ and inverting the premultiplying term of $dq$ yields

$$dx = -J_q(q_o)\,[\, K_q + \Delta(q_o, f)\,]^{-1}\, J_q^T(q_o) df \,. \tag{17}$$
$$\triangleq -K_x^{-1} df$$

Therefore, the taskspace stiffness $K_x$ is written by

$$K_x = \{\, J_q(q_o)\,[\, K_q + \Delta(q_o, f)\,]^{-1}\, J_q^T(q_o)\,\}^{-1} \,. \tag{18}$$

Finally, assuming $G(q)$ is the joint torque equivalent to the gravity force acting on the links of the manipulator, Eqs. (15) and (18) will be changed to

$$K_q = J_q^T(q_o) K_x J_q(q_o) - \Delta(q_o, f) - \Delta_g(q_o, f_g) \,. \tag{19}$$
$$K_x = \{J_q(q_o)[K_q + \Delta(q_o, f) + \Delta_g(q_o, f_g)]^{-1} J_q^T(q_o)\}^{-1} , \tag{20}$$

where $f_g$ denotes the gravity force, and $\Delta(\cdot,\cdot)_g$ is ISOC induced by the gravity force such as

$$\Delta_g(q_o, f_g) = \frac{\partial G(q_o)}{\partial q} \,. \tag{21}$$

Now, we define $K_{qe} \triangleq K_q + \Delta(q_o, f) + \Delta_g(q_o, f_g)$ and examine Eqs. (19) and (20). It is noticed from Eq. (20) that the effective stiffness at the joint appears to be $K_{qe}$. $K_{qe}$ is the actual stiffness to determine the responsive torque for the joint disturbances and thus, the stability of joint configuration depends on $K_{qe}$. Remembering that the stability of elastic system is determined by the positive definiteness of the stiffness matrix, it is stated that ISOC may lead the system to unstable state, while the stable joint servo stiffness is given. Secondly, if the joint servo stiffness is specified by Eq. (19), ISOC is compensated at the joint and the effective stiffness at the joint will be that of the conventional stiffness model. Therefore, the stiffness control problem can be treated in the same way as the previous ones that is going to be discussed in the next section.

# 3 Orthogonal Stiffness Decomposition Control

In the previous section, we presented a new stiffness model to describe the relations among the exerting force and the corresponding stiffnesses. Eq. (20) offers *forward stiffness computation model* and Eq. (19) does *backward stiffness computation model*, that is, *stiffness control model*. Based upon these formulation, a stiffness control method named *orthogonal stiffness decomposition control*(OSDC) is proposed, which provides a proper way to compensate ISOC and specify null stiffness.

Let us suppose that the manipulator at initial configuration $q = q_o$ is deflected and exerts the end effector force $f$. If the joint stiffness is specified by Eq. (19) such as

$$K_q = J_q^T(q_o) K_x J_q(q_o) - \Delta(q_o, f) - \Delta_g(q_o, f_g) \,,$$
$$= \hat{K}_q - \Delta(q_o, f) - \Delta_g(q_o, f_g) \,, \tag{22}$$

where $\tilde{K}_q \triangleq J_q^T(q_o) K_x J_q(q_o)$. Then, the effective servo stiffness at the joint will be

$$K_{qe} = J_q^T(q_o) K_x J_q(q_o) , \quad (23)$$

and it can be perceived that the stiffness model comes to the conventional one. Now, the behavior of the manipulator depends upon the characteristic of $\tilde{K}_q$ but it is known to be singular in the case of redundant manipulator. The problem comes to the derivation of a positive definite joint servo stiffness $\tilde{K}_q$ resulting in the specified taskspace stiffness, that is, the specification of null stiffness. In this paper, we employ the following method of computing the null stiffness[5].

If $\tilde{K}_q$ is decomposed by using similarity transform[11], a diagonal matrix $\Lambda_p$ having eigenvalues as its diagonal elements is obtained.

$$\Lambda_p = H^T \tilde{K}_q H , \quad (24)$$

$$= \mathrm{diag}(\lambda_1, \lambda_2, \cdots, \lambda_n) , \quad (25)$$

where the columns of the orthogonal matrix $H$ ($H^{-1} = H^T$) are the eigenvectors corresponding to eigenvalues $\lambda_1, \lambda_2, \cdots \lambda_n$ of $\tilde{K}_q$, respectively and

$$\lambda_1 \geq \lambda_2 \geq \cdots \geq \lambda_N \geq \lambda_{N+1} = \cdots = \lambda_n = 0 . \quad (26)$$

Here, a new matrix $\Lambda_h$ is defined with the non-zero diagonal elements $\tilde{\lambda}_i > 0$ $(N+1 \leq i \leq n)$ instead of zero diagonals for Eq. (25).

$$\Lambda_p = \mathrm{diag}(0, 0, \cdots, \tilde{\lambda}_{N+1}, \cdots, \tilde{\lambda}_n) , \quad (27)$$

Even if the zero eigenvalues $\lambda_i$ $(N+1 \leq i \leq n)$ is shifted to arbitrary positive values $\tilde{\lambda}_i$ the orthogonal matrix $H$ remains the same, since the matrix $\Lambda_h$ is always orthogonal to the matrix $\Lambda_p$. Thus, a new diagonal matrix $\Lambda$ is defined as the summation of $\Lambda_p$ and $\Lambda_h$.

$$\Lambda = \Lambda_p + \Lambda_h , \quad (28)$$

If $\Lambda$ is transformed reversely, the result consequently comes to be

$$\tilde{K}_q = J_q^T K_x J_q + K_n , \quad (29)$$

where $K_n \triangleq H \Lambda_h H^T$. Finally, the complete joint stiffness is obtained by

$$K_q = J_q^T K_x J_q + K_n - \Delta(q_o, f) - \Delta_g(q_o, f_g) . \quad (30)$$

The matrix $K_n$ enables us to directly assign new nonzero eigenvalues $\tilde{\lambda}_i$ $(N+1 \leq i \leq n)$ in the direction perpendicular to the hyperplane in which $K_{qe}$ lies. The $\tilde{\lambda}_i$'s determine the magnitude of the null motion stiffness in the direction of redundancy, which corresponds to the remaining eigenvectors of the matrix $H$.

While the intended operation of this controller is in contact with environment there are situations where we operate out of contact with it. It is therefore necessary to add damping effect and in the same way the taskspace stiffness is specified, we introduce the individual joint damping $K_{qd} \in \Re^{n \times n}$ such as

$$K_{qd} = \alpha H \, \mathrm{diag}(\lambda_1, \lambda_2, \cdots, \lambda_n) H^T , \quad (31)$$

where $\alpha$ is a scalar scale coefficient and determines the strength of damping. Therefore, the final form of the applied torque is given by the expression

$$\tau = K_q(q_o - q) + K_{qd}(\dot{q}_o - \dot{q}) + J_q^T f_o , \quad (32)$$

where $\dot{q}_d$ and $\dot{q}$ are the desired and current joint velocity, respectively.

# 4 Experimental Verification

To examine the effectiveness of the proposed approach, several experiments were performed using a planar three-dof redundant manipulator.

## 4.1 Outline of Experimental Setup

The manipulator was configured as a planar three-link structure and moved on the plane orthogonal to the gravity field as illustrated in Fig. 2, whose length $\ell_1$, $\ell_2$ and $\ell_3$ are given by 106, 65, 65 mm respectively.

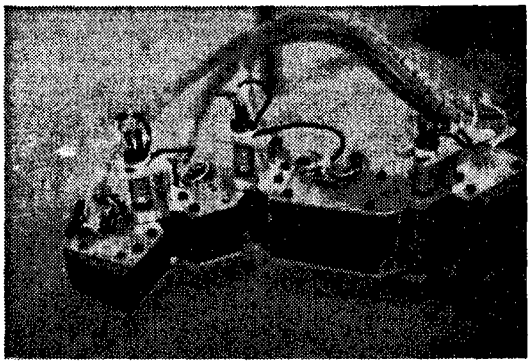

Figure 2: Three-dof redundant manipulator

The three joints were remotely actuated via tendons, where six torque controlled DC servo motors(rated torque 1.4Nm, torque constant 2.1Nm/A, and rated speed 60 rpm including harmonic reduction gear of 50:1), were used to provide commanded tensions for the tendons. The overall system architecture is illustrated in Fig. 3.

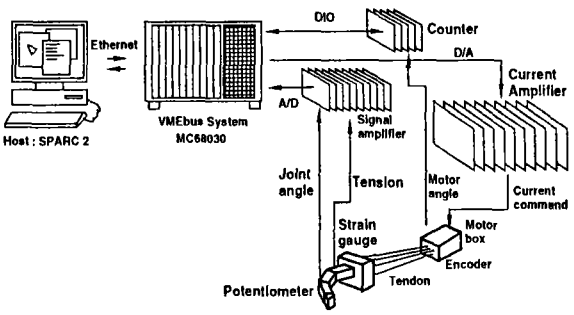


Figure 3: Overall system architecture

Hardware was composed of two 68030 based single board computers( Motorola MC68030 CPU ) with floating point unit in a VMEbus card cage, and SUN/SPARC workstation was used as a host computer. It had a D/A converter with 16 channels and a A/D converter with differential 16 channels to interface with sensors. Joint positions were measured by potentiometers directly attached at the joints, and joint torques were computed by measured tensions and the tension and torque relationship of coupled tendon driven system[9]. The controllers were implemented discretely, and control programs were written by C language with a few 68030 assembly codes. They were developed on a workstation in UNIX environment using a commercial realtime software development tool of VRTXvelocity[12]. The actuator level control and stiffness control loop ran at 400Hz and 100Hz, respectively.

### 4.2 Experiments

In the first experiment, the effect of ISOC was verified. We let the tip of manipulator contacted with a single axis force sensor(Bongshin load cell, 20kgf) and 2N bias force was given. In this situation, the depth of contact was increased about 0.06m very slowly along contact surface of the force sensor, expecting to exert the static contact force corresponding to the displacement offset similar to Fig. 1. The taskspace stiffness was given by

$$\boldsymbol{K}_x = \mathrm{diag}(\,100,\ 100\,)\,. \tag{33}$$

To verify ISOC proposed in our stiffness model, two control methods were applied: the one used the conventional control method, that is, the joint stiffness control without compensating ISOC, and the other was the proposed one, which compensated ISOC. In the proposed controller, the eigenvalue of null stiffness was set to be

$$\lambda_3 = 0.045\,. \tag{34}$$

Thus, the joint stiffness became

$$\boldsymbol{K}_q = \boldsymbol{J}_q^T \boldsymbol{K}_x \boldsymbol{J}_q + \boldsymbol{H}\ \mathrm{diag}(\,0,\ 0,\ 0.045\,)\ \boldsymbol{H}^T - \Delta(\boldsymbol{q}_o, \boldsymbol{f})\,. \tag{35}$$

Also, we specified the damping matrix as

$$\boldsymbol{K}_{qd} = 0.2\ \boldsymbol{H}\ \mathrm{diag}(\,\lambda_1,\ \lambda_2,\ \lambda_3\,)\ \boldsymbol{H}^T\,, \tag{36}$$

where $\lambda_1$, $\lambda_2$ and $\lambda_3$ are the eigenvalues of joint stiffness matrix $\boldsymbol{K}_q$.

Beforehand, we computed the minimum eigenvalues of the effective joint stiffness using Eq. (20) for the two control methods. As shown in Fig. 4, the minimum eigenvalue of the conventional controller came to be less than zero. It means that though the stable joint stiffness was specified in the conventional control method, the effective joint stiffness became negative definite due to ISOC and the configuration of the manipulator was expected to be unstable.

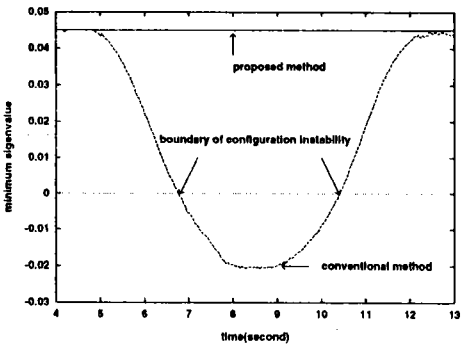


Figure 4: Minimum eigenvalues of the effective joint stiffness

It could be observed in Figs. 5, 6 and 7, which show the configuration of the manipulator during the experiments. Here, the desired configuration represents that of minimum potential energy. To determine the desired configuration of the manipulator, we introduced the following performance function

$$H(\boldsymbol{q}) = \frac{1}{2}(\boldsymbol{q} - \boldsymbol{q}_o)^T \boldsymbol{K}_q (\boldsymbol{q} - \boldsymbol{q}_o)\,. \tag{37}$$

Using the technique proposed in [10], we computed the desired joint configuration of satisfying the constraints of end effector position and minimum potential energy. As illustrated in these figures, conventional controller couldn't preserve the configuration of the manipulator and its configuration was far from the desired one. On the contrary, the manipulator showed stable behavior and also close to the desired one during the experiments. The effect of ISOC could be apparently perceived in the data of contact forces. The desired contact force is going to be the summation of bias force and force generated by stiffness such as

$$\boldsymbol{f}_d = \boldsymbol{K}_x(\boldsymbol{x} - \boldsymbol{x}_o) + \boldsymbol{f}_o\,, \tag{38}$$

where $\boldsymbol{f}_d$ is the desired contact force. As given in Fig. 8, the experimental results employing the conventional method could not track the desired force trajectory and the proposed controller exerted the desired static force successfully shown in Fig. 9.

In the second experiment, the compliance behavior of the manipulator was tested. The manipulator was driven along the planned trajectory with given taskspace stiffness. Along the traveling path, the manipulator was enforced to contact with the environment intentionally and the contact force was measured. The force sensor used in the first experiment, was placed in the taskspace parallel to the X-Y plane as shown in Fig. 10, and the nominal trajectory was given as a circular trajectory with 0.01 $m$ radius and 0.1 Hz period, low enough to neglect the inertial effect. Similar to the first experiment, two control methods were applied: the compensated controller of ISOC and the other without compensating it. The taskspace stiffness was given by

$$\boldsymbol{K}_x = \mathrm{diag}(\,400,\ 400\,)\,. \tag{39}$$

and the eigenvalue of null stiffness was set to be $\lambda_3 = 0.045$ and $\alpha$ to determine the strength of damping was 0.2.

The traveling paths of the end effector during the experiments are illustrated in 12 and 11. It could be observed that as the deflection gets larger the manipulator was hard to keep track of the nominal trajectory. We noticed the similar fact in the plots of measured contact forces given in Figs. 14 and 13. The conventional control method showed poor tracking performance of force, and vice versa.

## 5 Conclusion

A compliance control method of redundant manipulators was proposed. Through stiffness modeling, we formulated the equations to describe the relations between force and stiffness, where a new terminology called *induced stiffness obtained from configuration change and force*(ISOC) was introduced. ISOC can be considered as the resultant effect of the static force expressed in terms of stiffness. The proposed control method based on the developed model, provided a feasible way of controlling stiffness of redundant manipulators. Through the experiments, we confirmed the importance of ISOC and the effectiveness of the proposed control method.

## References


[1] M. H. Raibert, and J. J. Craig, "Hybrid Position/Force Control of Manipulators," *Trans. ASME, Dynamic Systems, Measurements and Control*, Vol. 102, No. 6, 1981, pp. 126-133.

[2] N. Hogan,"Impedance Control: An Approach to Manipulation, Part 1,2,3," *Trans. ASME, Dynamic Systems, Measurement and Control*, Vol. 107, 1985, pp. 1-24.

[3] J. K. Salisbury, "Active Stiffness Control of Manipulator in Cartesian Coordinates," *Proc. IEEE 19th Conf. on Decision and Control*, pp. 95-100, 1980.

[4] M. Kaneko, N. Imamura, K. Yokoi and K. Tanie, "Direct Compliance Control of Manipulator Arms - Basic Concept and Application Examples", *Proc. of 2nd IFAC Symposium on Robot Control*, (Karlsruhe, FRG), pp. 365-370, 1988.

[5] J. O. Kim, P. Khosla, and W. K. Chung, "Static Modeling and Control of Redundant Manipulators," *Robotics & Computer-Integrated Manufacturing*, Vol. 9, No. 2, pp. 145-157, 1992.

[6] K. Yokoi, H. Mackawa and K. Tanie, "A Method of Compliance Control for a Redundant Manipulator", *Proc. IEEE/RSJ Int. Conf. on Intelligent Robots and Systems*, (Raleigh, NC), pp. 1927–1934, 1992.

[7] F. A. Mussa-Ivaldi, and N. Hogan,"Integrable Solutions of Kinematic Redundancy via Impedance Control," *Int. J. Robotics Research*, Vol. 10, No. 5, pp. 481–491, 1991.

[8] B. J. Yi, D. Tesar, and R. A. Freeman, "Geometric Stability in Force Control," *Proc. IEEE Int. Conf. on Robotics and Automation*, (Sacramento,CA), pp. 281–286, 1991.

[9] S. Hirose, and S. Ma,"Coupled Tendon-driven Multijoint Manipulator", *Proc. IEEE Int. Conf. on Robotics and Automation*, (Sacramento,CA), pp. 1268–1275, 1991.

[10] P. H. Chang, "A Closed-Form Solution for Inverse Kinematics of Robot Manipulators with Redundancy," *IEEE J. Robotics and Automation*, Vol. RA-3, No. 5, pp. 393–403, 1987.

[11] G. Strang, *Linear Algebra and Its Applications*, Harcourt Brace Jovanovich, San Diego, 1988.

[12] Ready Systems Inc., *Manual of VRTXvelocity, realtime O/S*, 1991.

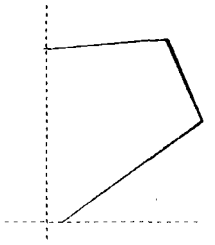

Figure 5: Desired configuration of manipulator

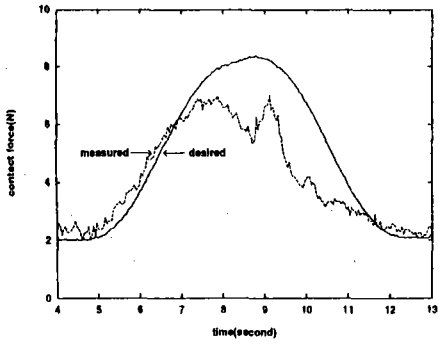


Figure 8: Contact force of conventional controller

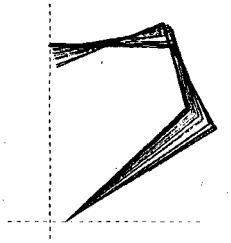

Figure 6: Configuration of manipulator by conventional controller

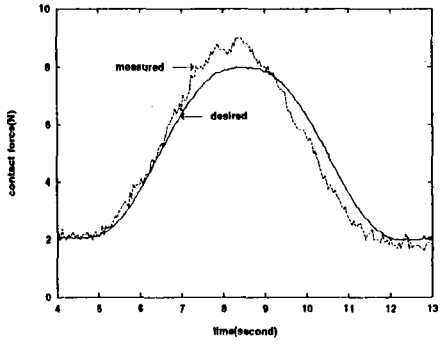


Figure 9: Contact force of proposed controller

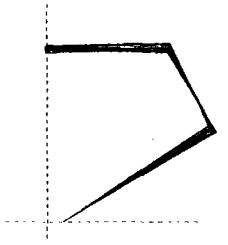

Figure 7: Configuration of manipulator by proposed controller

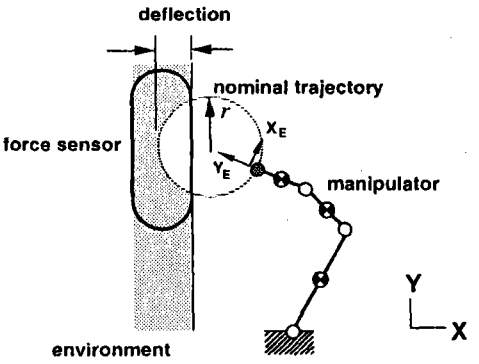


Figure 10: Schematic of experiment

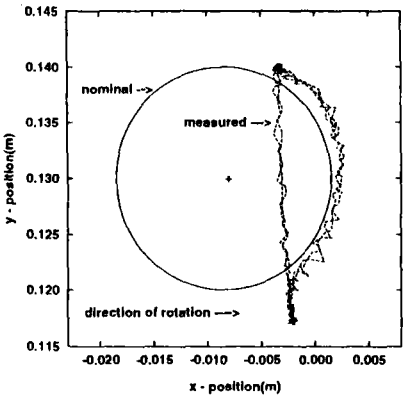


Figure 11: Contact motion trajectory of conventional control method

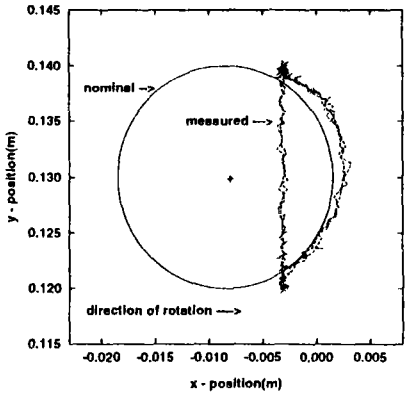


Figure 12: Contact motion trajectory of proposed control method

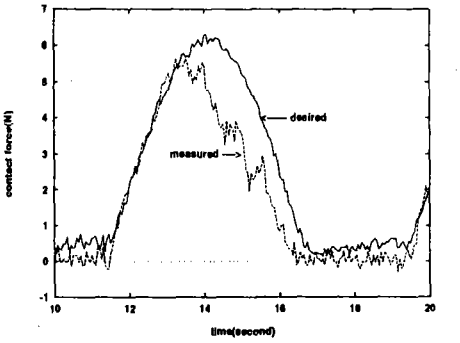


Figure 13: Measured contact force of conventional control method

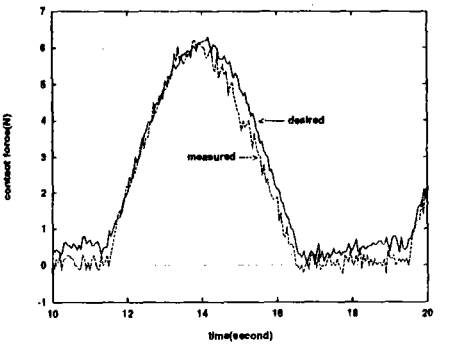


Figure 14: Measured contact force of proposed control method